Dynamics of Copolymer Micelles in a Homopolymer Melt: Influence of the Matrix Molecular Weight

Kerstin Gohr and Wolfgang Schärtl*

Institut für Pysikalische Chemie, Universität Mainz, Welderweg 11, 55099 Mainz, Germany

Received October 25, 1999; Revised Manuscript Received January 18, 2000

ABSTRACT: We have studied the dynamics of styrene−isoprene (SI) block copolymer micelles in a matrix of linear entangled polyisoprene (PI) chains, using forced Rayleigh scattering (FRS) and dynamic mechanical analysis (DMA). The molecular weight of PI has been varied from 22.000 g/mol, where the copolymer corona should be strongly swollen by the matrix chains (wet brush), to 50.000 g/mol, where corona swelling should be neglectable (dry brush). The diffusion coefficients determined by FRS showed a slowing down with increasing copolymer concentration, which is more pronounced in the case of the wet brush system. Comparing the diffusion mobility with hard-sphere colloids as a reference, a volume swelling ratio as a function of copolymer concentration and matrix molecular weight could be estimated. Surprisingly, the FRS experiments yield unusual decay−grow−decay signals for samples with very high copolymer amount. For these samples, which in analogy to colloidal hard spheres are close to the crystallization transition regime, the photobleaching process may cause a structural change, leading to complementary grating effects in the FRS signals. Further, DMA showed that the terminal relaxation process previously identified as micellar diffusion disappears for these highly concentrated samples, and an elastic plateau is obtained.

Introduction

Spherical block copolymer micelles in a homopolymer matrix behave, in some respects, analogous to dispersions of colloidal spheres in a molecular solvent.[1] For example, they form a cubic crystalline structure at high micellar concentration.[2,3] Concerning the particle dynamics, it recently has been found[4] that the hydrodynamic radius of rotation of an individual micelle in an entangled polymer matrix is nearly independent of micellar concentration and closely corresponds to the geometrical dimensions of the micelle, further indicating that block copolymer micelles in an entangled homopolymer melt behave more like compact colloidal particles than like hyperbranched or starlike polymers.

For colloidal systems, the interaction pair potential dominates the phase behavior, i.e., colloidal stability, crystallization etc., as well as the concentration dependence of the particle dynamics. For copolymer micelles in a homopolymer melt, Leibler and Pincus[5] have theoretically deduced a repulsive potential which, for a given copolymer, should depend on the matrix molecular weight: low molecular weight homopolymer leads to a strong swelling of the micellar corona (wet brush) and, consequently, to a long-range soft−repulsive interparticle interaction. This system is quite similar to charged spherical colloids in an aqueous solution, which also exhibit a long-range soft−repulsive interaction pair potential.[6,7] On the other hand, the micellar corona is much less swollen in the case of a matrix homopolymer of higher molecular weight (dry brush). Here, the repulsive interaction potential is short-ranged and expected to be steeper than in the case of the wet-brush system. Therefore, the dry-brush system closely resembles hard-sphere colloidal particles.[1,8−11] In Figure 1, a qualitative sketch of this effect of matrix homopolymer molecular weight on the intermicellar interaction pair potential is shown.

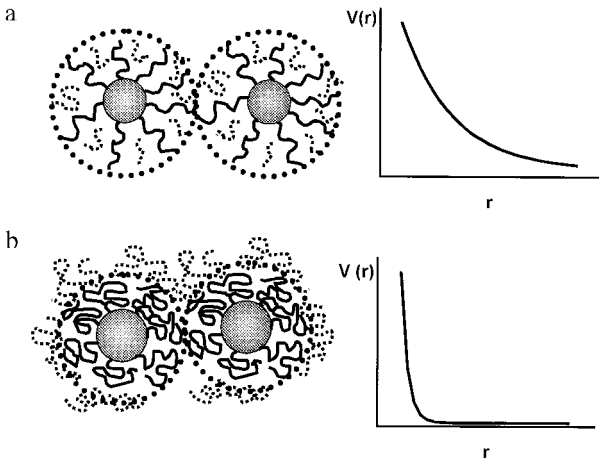

Figure 1. Sketch of the interaction pair potential between individual micelles with, in the case of low molecular weight homopolymer, strongly swollen corona (a, wet brush) and in the case of high molecular weight homopolymer, nonswollen corona (b, dry brush).

This fact that the range and steepness of the repulsive interaction potential can be adjusted continuously via the molecular weight of the matrix polymer makes copolymer micelles a very interesting colloidal model system.

As mentioned above, the concentration dependence of the particle diffusion may provide a measure for the range of particle interactions. Using hard spheres as a reference, an effective particle concentration can be determined which, in the case of long-range soft−repulsive potentials, can be much larger than the volume fraction calculated from the sample composition. For example, whereas hard spheres undergo a phase transition to a cubic crystalline structure at a volume fraction of about 0.50,[1] highly charged colloids in aqueous dispersion may already crystallize at compostion volume fractions lower than 0.01. Importantly, even charged particles can be described as effective hard

* To whom correspondence should be addressed. E-mail schaertl@mail.uni-mainz.de.

10.1021/ma991776r CCC: $19.00 © 2000 American Chemical Society
Published on Web 03/03/2000

Table 1. Characteristics of Block Copolymer and Homopolymers

sample code	M_n [g/mol]	M_w/M_n	wt % PS
SI	64 800	1.04	20.7
PI23k	22 100	1.02	0
PI47k	46 400	1.02	0
PI50k	49 400	1.05	0

spheres; i.e., the compositional particle concentration can be rescaled to an effective hard-sphere volume fraction by multiplication with a factor that remains nearly constant over the whole concentration regime.

In practice, an exact matching of the single-particle dynamics of charged colloids and hard-sphere systems at indentical effective volume fractions is not possible due to a difference in hydrodynamic interactions.[12] Here, one has to consider that both direct interactions between colloidal particles mediated by the interparticle pair potential and indirect hydrodynamic coupling, i.e., the influence of the motion of a given particle on a neighboring particle exerted by the surrounding medium, play an important role in the overall particle mobility. The latter depends strongly on the interparticle distance and therefore, at identical effective volume fraction, has to be different for charged colloids and hard-sphere systems.

For colloidal particles in a molecular solvent, the solvent molecules exerting a Brownian and a friction force on the much larger particles, and mediating the hydrodynamic coupling between them, are treated as a continuum (coarse graining).[1] For copolymer micelles in a homopolymer melt, such a coarse graining approach for the surrounding medium, i.e., the homopolymer chains whose size is not very much smaller than that of the micellar particles, seems to be inappropriate. Therefore, it is interesting to investigate in what respect copolymer micelles resemble common colloidal dispersions, especially concerning interparticle interaction potential and hydrodynamic contributions to the single-particle mobility.

In this paper, we try to address this problem by investigating the dynamics of styrene−isoprene (SI) copolymer micelles in a polyisoprene (PI) homopolymer melt for various concentrations and three different matrix polymers, ranging from $M = 22.000$ g/mol (wet brush) to 50.000 g/mol (dry brush). To complete the limited range of matrix molecular weights of our systems, we also had to rely on previous studies of the dynamics of SI micelles in a PI matrix of very low molecular weight, i.e., 5.000 g/mol, by Watanabe et al.[13] All diffusional mobilities measured by forced Rayleigh scattering (FRS) will be analyzed according to free volume theory[14] and with respect to an experimental hard-sphere reference system,[15] trying to obtain a semiquantitative measure for the range of the interparticle interactions as well as for the corona swelling of the individual micelle.

Experimental Section

Materials.The synthesis of the styrene−isoprene (SI) block copolymer containing the photoreactive dye *o*-nitrostilbene (ONS[16]) at the PS chain end and of the polyisoprene (PI) homopolymers used in these studies has been described in detail before.[4,17] Table 1 summarizes the sample characteristics, and Table 2 shows the matrix viscosities of the different homopolymers for the temperatures used during our diffusion measurements. The latter, which have been obtained by rheological measurements of the pure matrix polymers, are needed to calculate the hydrodynamic radii of the micelles (see below).

Table 2. Matrix PI Viscosities vs Temperature

sample code	η(40 °C) [Pa s]	η(95 °C) [Pa s]	η(120 °C) [Pa s]
PI23k	50.8	4.5	2.2
PI47k	187.9	17.3	8.8
PI50k	413.8	75.5	37.4

As previously, copolymer/homopolymer blends containing micelles with glassy S-core and fluid I-corona embedded in a fluid PI matrix were prepared by solvent casting from cyclohexane solution. Remaining cyclohexane was removed by vacuum annealing at 60 °C for 3 days.

Forced Rayleigh Scattering. Self-diffusion coefficients of dye-labeled spherical micelles in a homopolymer melt have been determined using a standard FRS setup in amplitude grating mode as described elsewhere.[4,17] The typical exposure time for the holographic writing process was 25 ms, at laser power 100 mW. In the case of one simple translational diffusion process, the signal measured by the FRS experiment is described by

$$I(t) = \left[A \exp\left(-\frac{t}{\tau}\right)\right]^2 + C \tag{1}$$

A is the amplitude of the diffraction signal immediately after photobleaching, τ the diffusional relaxation time, and C the scattering background contributing incoherently to the FRS intensity and therefore identical to the scattering measured before photobleaching. The translational self-diffusion coefficient D_s is determined from the relaxation time according to

$$D_s = \frac{d^2}{4\pi^2\tau} \tag{2}$$

Here, d is the periodic lattice spacing of the holographic grating, which depends on the wavelength λ of the laser and the bleaching angle 2θ:

$$d = \frac{\lambda}{2\sin(\vartheta)} \tag{3}$$

$$q = \frac{2\pi}{d} \tag{4}$$

q is the length of the scattering vector of the FRS experiments. Its magnitude is proportional to $\sin(\theta)$ and therefore reciprocal to the holographic lattice spacing d.

In the case of rotational motion of labeled tracer particles contributing to the FRS signal, a double-exponential decay can be obtained:

$$I(t) = \left[A_1 \exp\left(-\frac{t}{\tau_1}\right) + A_2 \exp\left(-\frac{t}{\tau_1}\right)\right]^2 + C \tag{5}$$

with A_1 and A_2 the amplitudes and τ_1 and τ_2 the relaxation times of the first and second dynamical processes, respectively. If the first process corresponds to the rotational motion, the rotational diffusion coefficient is given by

$$D_{rot} = \frac{1}{6\tau_1} \tag{6}$$

whereas the translational diffusion coefficient is calculated from τ_2 according to eq 2. Here, it should be noted that, in a FRS experiment, the rotational relaxation time, in contrast to the translational relaxation time, is independent of the holographic lattice spacing d. Analysis of the d dependence of the relaxation rate of a given process therefore allows to determine whether it is either localized (rotational) motion or translational diffusion.

Provided that the light absorption in the bleached areas of the holographic lattice immediately after photobleaching is nonzero, different relaxation rates of tracer particles in the

bleached and nonbleached zones may cause even more complicated FRS signals. These signals with grow−decay or even decay−grow−decay shape are explained by a so-called complementary grating scenario[18] and can be analyzed according to

$$I(t) = \left[A_1 \exp\left(-\frac{t}{\tau_1}\right) + A_2 \exp\left(-\frac{t}{\tau_2}\right)\right]^2 + C \qquad (7)$$

with A_1 and τ_1 the amplitude and relaxation time of the amplitude grating formed by the tracer particles of the nonbleached regions and A_2 and τ_2 the amplitude and relaxation time of the complementary grating formed by tracer particles of the bleached regions. At very high block copolymer concentrations, our FRS signals had to be analyzed using eq 7 (see below and ref 17).

FRS samples were prepared at room temperature by cold pressing between two optical disk-shaped glass plates with diameter 2 cm. The sample thickness was adjusted to 0.1 mm by Teflon spacers. All samples were annealed at the measurement temperature for 6 h prior to the first diffusion measurement. This annealing period allows for relaxation of convectional or pressure-induced flow processes, which lead to regular oscillations in the FRS decaying signals.

Mechanical Spectroscopy. Dynamic mechanical measurements have been performed using a Rheometrics RMS 800, with plate−plate geometry and variable plate diameters (6 and 13 mm). The samples were subjected to small oscillatory shear strain, and the resulting stress was measured. Master curves for the real (G') and imaginary (G'') parts of the dynamic complex shear modulus have been obtained using the time−temperature superposition principle (i.e., shifting the data recorded at various temperatures only along the frequency coordinate).[19]

Results and Discussion

Like in our previous experiments,[4,17] the FRS measurements have been performed at different temperatures all well below T_{ODT}, above which the micelles dissolve into isolated block copolymer chains. As already found for the dry-brush system (PI50k[4]), the micelles studied here in different matrix homopolymers also revealed two relaxation processes at the lowest temperature $T = 40$ °C. The fast process was independent of the scattering vector **q**, whereas the relaxation time of the slower process scaled linearly with q^{-2}. Therefore, like in our former work, the faster process has been attributed to micellar rotation and the slower one to translational diffusion of micelles. Here, it is important to note that rotation of the micelles can only be detected because the labels, which are stuck inside the glassy PS core, are not able to reorient independently of the whole micelle. At higher temperatures close to the glass transition of the PS core (i.e., T ca. 80 °C), where usually signals with higher amplitude are obtained due to an increase in efficiency of the photobleaching process, the rotational process becomes too fast for detection and/or disappears because of the enhanced reorientation capability of individual dye labels within the softened micellar core.

In Figure 2, we have plotted the translational self-diffusion coefficients determined at $T = 95$ °C for three different matrix homopolymers, i.e., 23k, 47k, and 50k, versus compositional block copolymer volume fraction. The latter has been calculated from the weight composition of the samples, assuming bulk polymer densities $\rho_{PS} = 1.053$ g/mL and $\rho_{PI} = 0.913$ g/mL. Also shown are the data by Watanabe et al.[13] with PI5k and $T = 30$ °C. In analogy to the concentration dependence of the dynamics of colloidal hard spheres, we have tried to fit all these data with the so-called Doolittle equation,

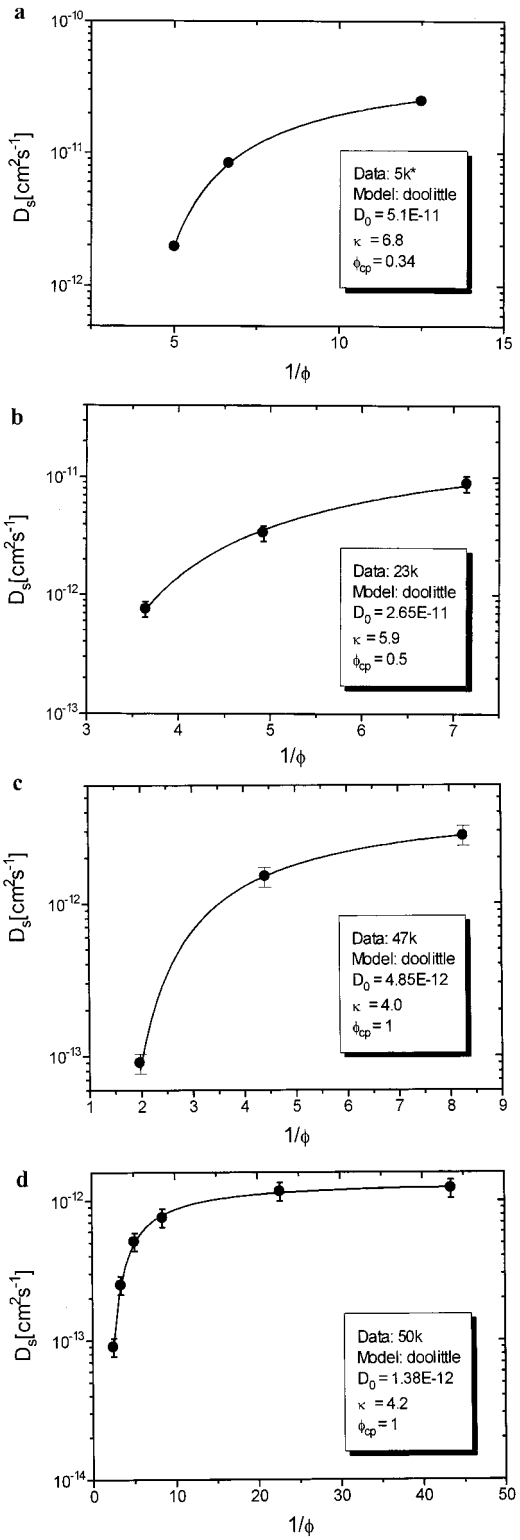

Figure 2. Self-diffusion coefficients of micelles as a function of micellar volume fraction for four different matrix homopolymers (a, PI5k (from ref 13); b, PI23k; c, PI47k; and d, PI50k). Lines are exponential fits according to the phenomenological free volume theory (Doolittle equation, see eq 8).

which is based on free volume theory:[14]

$$D = D_0 \exp\left(-\frac{\kappa}{\frac{1}{\varphi} - \frac{1}{\varphi_{cp}}}\right) \qquad (8)$$

Here, κ is a measure for the strength of a colloidal glass

Table 3. Hydrodynamic Radii (in nm) of Rotation (T = 40 °C) and Translation (T = 95 °C) As Determined from Debye and Stokes−Einstein Equations and Matrix PI Viscosities, Respectively

matrix	R_{rot} [10% SI]	R_{rot} [20% SI]	R_{rot} [30% SI]	R_{rot} [40% SI]	R_{trans} [SI → 0]
PI23k		30	33		23
PI47k	27	26			32
PI50k	29	24	35		26

former, i.e., the smaller κ, the steeper the interparticle repulsion potential and the steeper the slowing down of particle mobility with increasing particle concentration. ϕ is the particle volume fraction, and ϕ_{cp} is the volume fraction of close packing, i.e., the particle concentration where the diffusion coefficient D becomes zero. For the experimental hard-sphere system studied previously,[15] these parameters were $\kappa = 1.6$ and $\phi_{cp} = 0.65$. Finally, the diffusion coefficient for ideally dilute systems, D_0, is given by the Stokes−Einstein equation:

$$D_0 = \frac{kT}{6\pi\eta R_{trans}} \tag{9}$$

kT is the thermal energy, η the viscosity of the matrix, and R_{trans} the translational hydrodynamic radius of the diffusing particle.

Analogously, the Debye equation describes the rotation of colloidal particles in dilute systems:

$$D_{rot,0} = \frac{kT}{8\pi\eta R_{rot}^{\ 3}} \tag{10}$$

with R_{rot} the hydrodynamic radius of rotational motion.

From the results of the exponential fits shown in Figure 2, D_0 of the micellar systems has been determined. Using eq 9, the translational hydrodynamic radius of the micelles has been calculated. On the other hand, the hydrodynamic radius of rotation has been calculated from the rotational relaxation times measured in the FRS experiments, using eqs 6 and 10. The effect of particle concentration on D_{rot} has been ignored in this case. All resulting hydrodynamic radii have been summarized in Table 3.

First, it should be noted that R_{rot} remains nearly constant within experimental error. On the other hand, R_{trans} determined from D_0 of the fits agrees, within experimental error, quite well with R_{rot}. Both radii are comparable to the dimensions of the micelle r = 28.5 nm as estimated from the unperturbed chain dimensions of the PS and the PI block, respectively.[4] Finally, it should be noted that no systematic effect of the PI matrix molecular weight on these radii could be detected. Here, it should be mentioned that the hydrodynamic radius of swollen micelles might be quite different from the geometric radius due to the possibility of matrix homopolymer draining through the strongly expanded corona.

However, the values for ϕ_{cp} determined from the fits shown in Figure 2, in comparison to the hard-sphere value ϕ_{cp} = 0.65 (0.64 for monodisperse systems!), provide a first estimate of the volume swelling of the individual micelles. Here, it should be noted that this procedure neglects the possibility that, for example due to interpenetration and/or corona deformation, the effective volume swelling ratio might depend on particle concentration. This possibility will be discussed in some detail further beyond. According to the fit results, the

Table 4. Hydrodynamic Radii R_{trans} (in nm) of Translation for T = 40, 95, and 120 °C As Determined from Stokes−Einstein Equation and Matrix PI Viscosities

matrix PI23k	14 vol % SI	20 vol % SI	28 vol % SI
40 °C	55	163	585
95 °C	68	180	803
120 °C	70	196	595

matrix PI47k	12 vol % SI	22 vol % SI
40 °C	51	102
95 °C	52	104
120 °C	55	121

matrix PI50k	12 vol % SI	20 vol % SI	29 vol % SI	39 vol % SI
40 °C	80	69	504	107
95 °C	47	70	143	396
120 °C	39	55	70	94

5k system studied by Watanabe et al.[13] exhibits a close packing volume fraction ϕ_{cp} = 0.34, corresponding to an effective volume swelling by a factor 0.65/0.34 = 1.9. Note, however, that the value for κ = 6.8 is much larger than the hard-sphere value of 1.6. This means that the particle mobility of the micellar system PI5k slows down much less steeply with increasing concentration compared to the case of the hard-sphere system. Since the close packing volume fraction provides a measure for the volume swelling at very high particle concentrations, this means that the swelling ratio at lower concentrations could be much larger than 1.9, indicating some interpenetration and/or deformation of the micellar corona with increasing concentration. For system PI23k, the volume swelling ratio is 0.65/0.5 = 1.3, whereas κ = 5.9. This indicates that system PI23k more closely resembles the hard-sphere system than the system PI5k; i.e., the swelling of the micellar corona is more pronounced for the shorter matrix, as expected and already sketched in Figure 1. For systems PI47k and PI50k, a very interesting result is found: here, ϕ_{cp} = 1.0, meaning that the close packing particle concentration is even higher than that of hard spheres. Whereas hard spheres even at close packing always possess some free volume, i.e., colloidal dispersions reach a glassy solid state at 65 vol % particle concentration and 35 vol % solvent, these copolymer micelles seem to maintain their mobility up to the pure system (matrix concentration 0 vol %). This only can be explained if the micellar corona deforms at very high concentrations to fill up the free volume left in nondeformable hard-sphere systems, a scenario which is more than plausible if one considers that both micellar corona and PI matrix are in a liquid state (polymer melt), and just the micellar core which is only about 20 vol % of the total copolymer concentration is solid (glassy polymer) and nondeformable. This also leads to a strong dependence of effective particle volume (and volume swelling with respect to a hard-sphere reference) on particle concentration, as will be investigated in more detail in the next paragraph. Finally, we should note that systems PI47k and PI50k, with κ around 4.0, in that respect still more closely correspond to the hard-sphere system than systems PI23k and PI5k.

Before this discussion is continued, a short comment concerning the effect of temperature on particle mobility should be given. Hydrodynamic radii calculated using

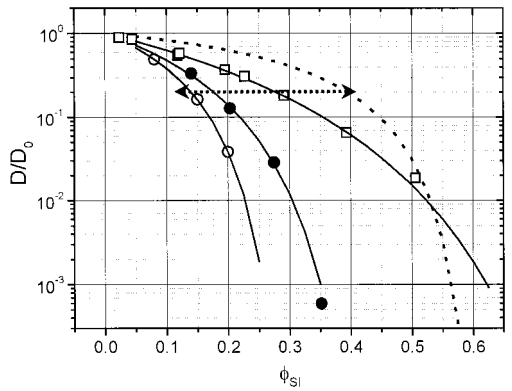

Figure 3. Normalized self-diffusion coefficients of micelles as a function of micellar volume fraction for matrix homopolymers PI5k (open circles, from ref 13), PI23k (filled circles), and PI47k/50k (open squares). The solid lines are guides to the eye, and the dotted line corresponds to experimental results for hard-sphere colloids dispersed in an organic solvent (from ref 15). The arrow indicates the determination of an effective hard-sphere volume fraction at identical reduced particle diffusivities, e.g., $\phi_{eff} = 0.40$.

the Stokes−Einstein equation and the matrix viscosities from Table 2 have been summarized in Table 4.

For all systems, the radii increase with increasing concentration, corresponding to the slowing down of the particle mobility D with respect to D_0. On the other hand, for identical systems the radii obtained at different sample temperatures are, within experimental error, nearly identical. This means that the particle mobility scales nicely with the viscosity of the matrix. Therefore, the characteristic slowing down in particle mobility with concentration discussed here for various micellar systems should not depend on temperature. Therefore, the choice of $T = 95$ °C to obtain a representative data set as a reference should be justified, and these data also should be comparable to the results from ref 13 obtained at $T = 30$ °C.

Figure 3 shows the diffusion coefficients (symbols) normalized by the D_0 values obtained from the exponential fits (see Figure 2) versus copolymer volume fraction for our three different systems and the system studied by Watanabe et al.[13] The data points corresponding to the highest particle concentrations of systems PI23k (35%) and PI47k (50%) have been obtained from unusual FRS signals (see below) and therefore are neglected in the fits of Figure 2. Also included are the fitting curves themselves (lines). As a reference to determine the effective hard-sphere particle volume fraction, diffusion coefficients of hard-sphere colloids in organic solution, i.e., polyorganosiloxane microgels dispersed in cyclohexane, obtained from dynamic light scattering and forced Rayleigh scattering,[15] have been added (dotted line). If we describe the micellar systems as effective hard-sphere colloids, all systems should have identical particle mobilities at identical effective particle volume fraction. This is indicated by the arrow in Figure 3 for an effective volume fraction of 0.40. In Table 5, we have compiled the compositional volume fractions of the micellar systems, i.e., the copolymer concentration, for effective hard-sphere volume fractions from 0.25 to 0.45. Here, it should be noted that the numbers given in Table 5 have been determined from a comparison of the particle mobilities calculated from the fitting curves directly, sampled with a volume fraction resolution of 0.005.

Table 5. Effective Hard-Sphere Volume Fractions and Swelling Ratios (in Parentheses) of Various Micellar Systems versus Concentration Determined as Shown in Figure 3

ϕ_{eff} (h.s.)	0.26	0.31	0.40	0.45
ϕ (PI5k[a])	0.08 (3.3)	0.10 (3.1)	0.14 (2.9)	0.17 (2.6)
ϕ (PI23k)	0.10 (2.7)	0.12 (2.6)	0.18 (2.2)	0.22 (2.0)
ϕ (PI50k)	0.14 (1.9)	0.18 (1.7)	0.28 (1.4)	0.36 (1.3)

[a] Data from ref 13.

If we divide the effective volume fraction by the compositional volume fraction, we obtain the volume swelling ratios given in parentheses in the table. As already indicated in the discussion of Figure 2, there is a distinct decrease in swelling ratio with increasing concentration. Therefore, copolymer micelles in a homopolymer matrix seem to behave quite different from hard-sphere colloids. The deviation could be caused by compression and/or deformation of the ultrasoft particles at very intense interparticle interactions found in the highly concentrated regime. To investigate this effect in more detail, neutron scattering studies to measure the micellar corona structure as a function of matrix molecular weight and copolymer concentration currently are in progress and will be presented in a subsequent publication. As also can be seen from the table, the swelling ratio decreases with increasing molecular weight of the matrix homopolymer, i.e., from wet brush (5k) to dry brush (50k). Finally, there is a remarkable crossover of hard-sphere reference and the PI50k system around $\phi = 0.55$. This also supports our previous assumption that the dry-brush system, due to deformation of the liquid corona, maintains some particle mobility up to zero matrix concentration (Figure 2, $\phi_{cp} = 1$). In contrast, the wet-brush systems (PI5k, PI23k) always contain a large amount of matrix homopolymer within the copolymer corona; therefore, even though the corona is also deformable, the close packing concentration ϕ_{cp} remains well below that of the hard-sphere system.

At the end of this article, we will discuss the dynamical results obtained for samples with very high copolymer concentrations. For the hard-sphere reference system, a phase transition from fluid to crystalline is found in the volume fraction regime $\phi = 0.50-0.54$.[1] As estimated from the swelling ratios given in Table 5, these effective hard-sphere volume fractions correspond to copolymer volume fractions of about 0.45−0.49 in the case of matrix PI50k and 0.29−0.32 in the case of PI23k. In Figure 4, FRS signals are shown for micellar systems with effective particle concentration in this hard-sphere colloidal crystallization regime.

Unusual decay−grow−decay signals are found in both cases. As discussed previously for the dry-brush system with matrix PI47k[17] and mentioned above, these signals are caused by complementary grating effects, i.e., a difference of particle mobilities in the bleached and nonbleached areas, respectively. As described in detail elsewhere,[17] we believe that this phenomenon is caused by a photoinduced phase transition. Before the bleaching process, the micellar arrangement even at high concentration is quite disordered, as shown in previous results of small-angle X-ray scattering (SAXS) measurements.[4,17,20] Crystallization of the micellar system due to the low mobility of the particles in the polymer melt can be expected to be a very slow process, which leads to a rather fluidlike structure even at high concentrations in the crystallization regime. This state, however,

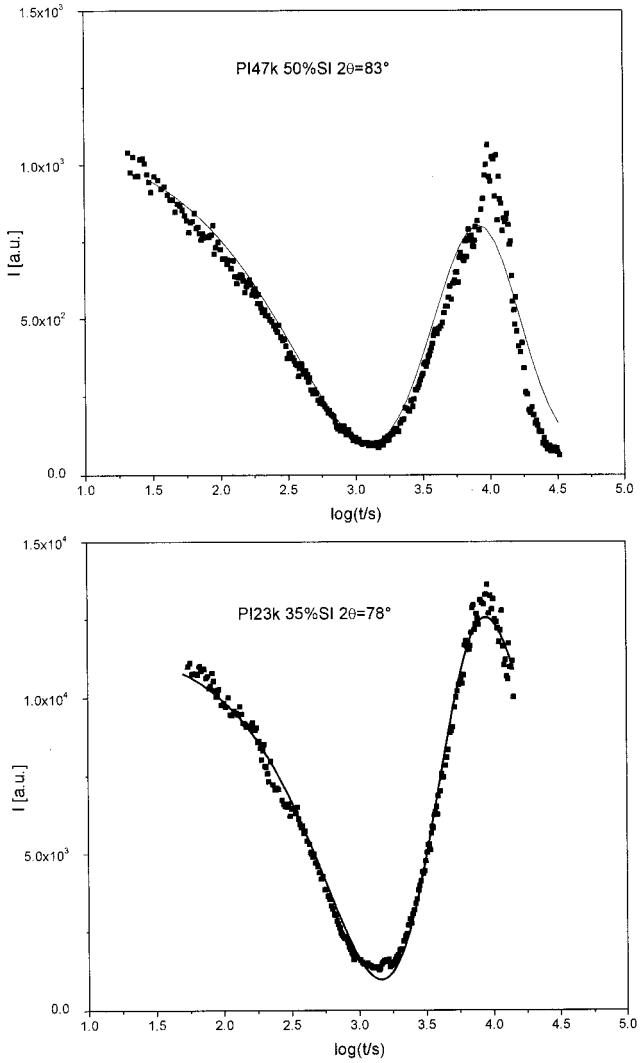

Figure 4. Decay−grow−decay FRS signals obtained at T = 95 °C for strongly interacting spherical micelles at very high concentrations, i.e., $\phi = 0.50$ for the dry-brush system[17] (PI47k) and $\phi = 0.35$ for the wet-brush system (PI23k). Lines correspond to best fits according to eq 8. See text for discussion.

is assumed to be metastable, and the energy input occurring during the bleaching process may enhance the probability of a crystalline particle arrangement. In these crystalline regions, the particle mobility should be greatly reduced in comparison to the nonbleached areas with a more fluidlike arrangement. Finally, it should be mentioned that the unusual decay−grow−decay FRS signals already have been obtained previously for samples containing 50 wt % copolymer micelles with PI core and PS corona in a PS homopolymer matrix.[21] We therefore conclude at present that this phenomenon of FRS complementary gratings is rather universal for systems in a metastable state undergoing a photoinduced phase transition. This problem will be discussed in more detail in a subsequent publication, investigating the effect of bleaching duration and laser power on the signals and especially trying to investigate the sample structure before and after macroscopic irradiation with laser light by SAXS.

Finally, it is interesting to note that a transition to unusual dynamic behavior at very high micellar concentrations also has been found in our dynamical mechanical measurements.

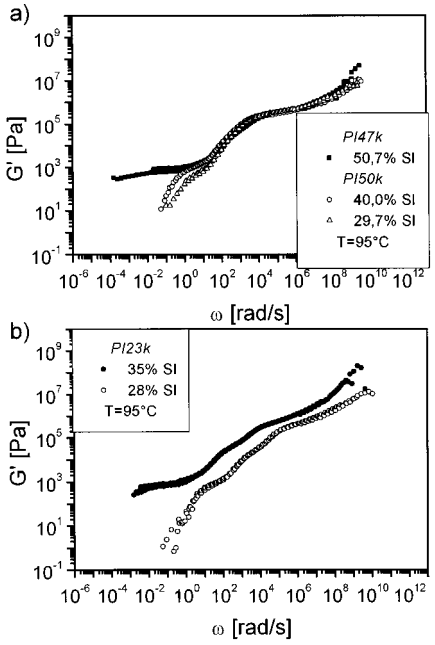

Figure 5. Concentration and frequency dependence of elastic moduli G' for dry-brush (PI47k, PI50k) and wet-brush (PI23k) systems. Note the occurrence of an elastic plateau (or disappearance of the terminal relaxation process) at high concentrations, where also unusual FRS signals have been found and a phase transition is assumed.

Figure 5 shows the storage modulus $G'(\omega)$ for the wet brush (PI23k) and dry brush (PI47k, PI50k) at various copolymer concentrations. As described previously,[4] the terminal relaxation process found at low frequency corresponds to micellar diffusion. Interestingly, this process disappears, and an elastic plateau is formed at high concentrations in the phase transition regime, where also the unusual FRS signals have been found. This is characteristic for a fluid−solid transition.

We therefore may conclude here that copolymer micelles in an entangled homopolymer matrix show a dynamical behavior analogous to colloidal hard spheres in the fluid regime. Further, the signature of a fluid−solid phase transition has been found in our dynamical studies at effective hard-sphere volume fractions corresponding exactly to the phase transition regime of the hard-sphere reference system.

Acknowledgment. We thank Y. Kanazawa and M. Schöps for synthesis of the polymers and C. Graf for preparation of the photoreactive label molecules. Also, we are very grateful to Prof. Sillescu for providing his FRS setup for these measurements. Helpful discussions with Dr. T. Pakula concerning the rheological measurements are also gratefully acknowledged. This work was financially supported by the Deutsche Forschungsgemeinschaft, Grant SCHA620/2-1.

References and Notes

(1) Pusey, P. N. In *Liquids, Freezing and the Glass Transition*; Les Houches Sessions LI.; Levesque, D., Hansen, J. P., Zinn-Justin, J., Eds.; Elsevier: Amsterdam, 1990. See also references therein.

(2) Hashimoto, T.; Fujimura, M.; Kawai, H. *Macromolecules* **1980**, *13*, 1660.

(3) Berney, C. V.; Cohen, R. E.; Bates, F. S. *Polymer* **1982**, *23*, 1222.

(4) Gohr, K.; Pakula, T.; Tsutsumi, K.; Schärtl, W. *Macromolecules* **1999**, *32*, 7156.
(5) Leibler, L.; Pincus, P. A. *Macromolecules* **1984**, *17*, 2922.
(6) Derjaguin, B. V.; Landau, L. *Acta Physiochem.* **1941**, *14*, 633.
(7) Verwey, E. J. W.; Overbeek, J. Th. G. *Theory of the Stability of Lyophobic Colloids*; Elsevier: Amsterdam, 1948.
(8) Alder, B. J.; Wainwright, T. E. *J. Chem. Phys.* **1957**, *27*, 1208.
(9) Alder, B. J.; Wainwright, T. E. *J. Chem. Phys.* **1970**, *53*, 3813.
(10) Woodcock, L. V.; Angell, C. A. *Phys. Rev. Lett.* **1981**, *47*, 1129.
(11) Schaertl, W. *Trends Stat. Phys.* **1998**, *2*. See also references therein.
(12) Banchio, A. J.; Nägele, G.; Bergenholtz, J. B. *J. Chem. Phys.*, in press.
(13) Watanabe, H.; Sato, T.; Osaki, K.; Hamersky, M. W.; Chapman, B. R.; Lodge, T. P. *Macromolecules* **1998**, *31*, 3740.
(14) Doolittle, A. K. *J. Appl. Phys.* **1951**, *22*, 1471.
(15) Graf, C.; Schärtl, W.; Maskos, M.; Schmidt, M. *J. Chem. Phys.*, in press.
(16) Splitter, J. S.; Calvin, M. *J. Org. Chem.* **1955**, *20*, 1086.
(17) Schaertl, W. *Macromol. Chem. Phys.* **1999**, *200*, 481.
(18) Spiegel, D. R.; Sprinkle, M. B.; Chang, T. *J. Chem. Phys.* **1996**, *104*, 4920.
(19) Ferry, D. J. *Viscoelastic Properties of Polymers*, 3rd ed.; Wiley: New York, 1980.
(20) Schaertl, W.; Tsutsumi, K.; Kimishima, K.; Hashimoto, T. *Macromolecules* **1996**, *29*, 5297.
(21) Hashimoto, T.; Funaki, K.; Schärtl, W.; Sillescu, H. *Polym. Prepr.* **1994**, *43*, 10.

MA991776R